



# CFD SIMULATION OF WIND EFFECTS ON INDUSTRIAL RCC CHIMNEY

**Mohd. Mohsin Khan**

Lecturer, Department of Civil Engineering, National Institute of Technology,  
Hamirpur, Himachal Pradesh, India

**Dr. Amrit Kumar Roy**

Assistant Professor, Department of Civil Engineering, National Institute of Technology,  
Hamirpur, Himachal Pradesh, India

## ABSTRACT

*The structural design considerations of a power station chimney are mainly governed by the effect of the wind loads. Wind tunnel studies become important to measure wind loads on the models of the chimney. It is very important to take the effect of interference in design of high rise structure for the serviceability purpose. It takes into account the variation of the mean wind velocity and turbulence parameters with height above the ground level. For the calculation of the wind loads and there effects; extensive wind tunnel testing is required. CFD offers a very powerful alternative to predict the wind related phenomena on chimneys or different kind of structures. A software package, FLUENT-14 (ANSYS 14.0) was used for CFD analysis. FLUENT-14 is a general CFD code based on the finite volume method and an algebraic multi-grid coupled solver.*

**Key words:** Chimney, Atmospheric boundary layer, Velocity profile, Turbulence intensity profile, Pressure distribution, Pressure coefficient, Velocity vector, CFD simulation

**Cite this Article:** Mohd. Mohsin Khan and Dr. Amrit Kumar Roy, CFD Simulation of Wind Effects on Industrial RCC Chimney. *International Journal of Civil Engineering and Technology*, 8(1), 2017, pp. 1008–1020.

<http://iaeme.com/Home/issue/IJCIET?Volume=8&Issue=1>

## 1. INTRODUCTION

In the era of industrial revolution, where the power sector mainly contributes to the development and improvement of the economy of a country, gives rise to the various sub-aspects which should be taken care of so as to minimize the various effects which may lead to environmental degradation. With the growing demand of power all around the world, grows the need of setting up of the power generation plants which in turn increases the demand of setting up of industrial chimneys. The main purpose of chimney is to disperse the toxic or flue gases at relatively high elevations minimizing the various environmental hazards it can cause when not dispersed properly. Industrial chimneys vary in size and shape from large power station reinforced concrete chimneys, which may be over 200 m in height and more than 20 m in diameter, to steel chimneys only a few tens of metres high and less than one metre

in diameter. Industrial chimneys due to their large height obstruct the wind flow and are subjected to extreme wind loads and hence the wind load is considered as one of the main design loads.

For estimating the design wind loads, codes provide some guidelines but are limited to some conventional geometry structures. Therefore for structures with unconventional geometry such as industrial chimneys, cooling towers, multi-storey high-rise buildings etc. wind tunnel testing is required and wind tunnel testing being expensive and also time consuming, CFD simulation is an alternative for the wind tunnel analysis. Several researchers have incorporated CFD simulation for the observation of wind effect on structures and the result obtained are found to be acceptable when compared with wind tunnel experiment.

Computational Fluid Dynamics (CFD) has been derived from different disciplines of fluid mechanics and heat transfer. CFD is particularly dedicated to fluids that are in motion, and how the fluid flow behavior influences processes that may include heat transfer and possibly chemical reactions in combusting flows. Additionally, the physical characteristics of the fluid motion can usually be described through fundamental mathematical equations, usually in partial differential form, which govern a process of interest are often called governing equation in CFD.

In order to solve these mathematical equations, they are converted using high level computer programming languages into computer programs or software packages which require high speed digital computers to attain the numerical solutions. These CFD Numerical solutions have significantly helped in obtaining the data like wind loads and moments acting on the structures. These wind loads and moments can be used, along with combination of dead loads and live loads (analysis done in STAAD. Pro), to find the extreme loading case.

## 2. DETAILS OF THE PROTOTYPE OF THE CHIMNEY

The details, as considered in this study of the prototype chimney and wind conditions of site for which models of chimney & other buildings have been prepared and wind tunnel simulation has been carried out by John, et al. (2012). The chimney is located in a power station which is comparatively in a flat region of the Panipat city, India. Within a radius of some 200 m it is surrounded by power station structures. The chimney design is of circular-ring cross-section. The outside diameter at the tip of the full-scale chimney is 13.6 m. From the tip to 60 m height of the chimney, the outside shell of the chimney is cylindrical. The outer diameter of chimney varies linearly with 1 in 38.125 tangential gradient from 60 m to the base of chimney.

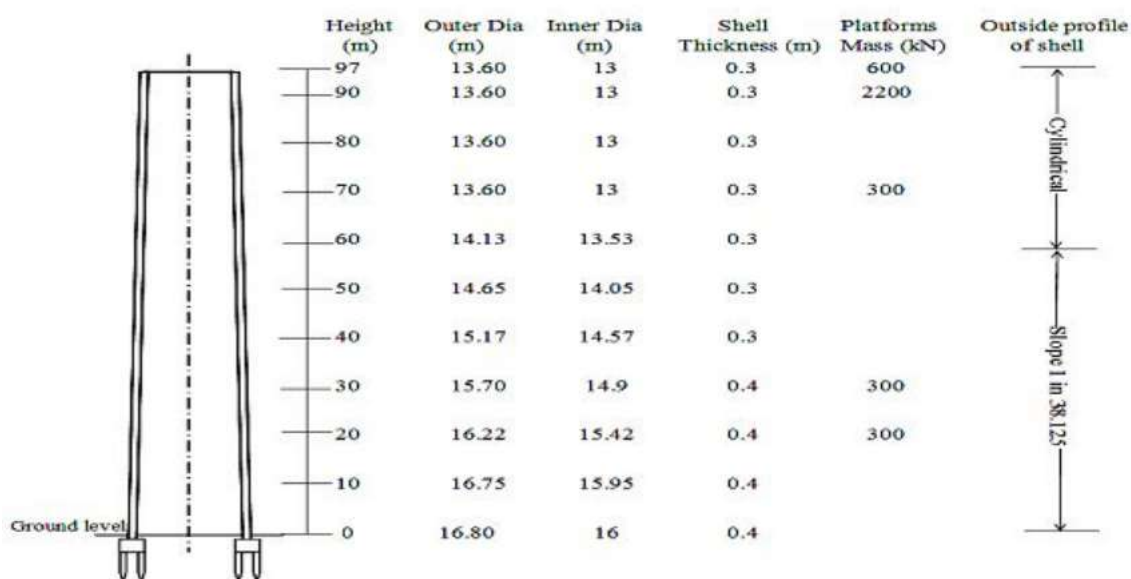


Figure 1 Shell and concentrated load profile of 97 m tall power station chimney

## 2.1. Modeling criteria & selection of geometric scale for the CFD study

The present research work aims at studying the wind effect on a power station chimney. A rigid model is used for the study. The geometric scale of model of a building is chosen to maintain the equality of ratios of overall building dimensions to the inherent lengths of the generated model wind. These inherent lengths may be roughness length of terrain, the boundary layer depth and the integral scale of the longitudinal component turbulence. Some other factors include the size of the test section and the ranges of parameters to be studied. In selecting the model scale it is important to avoid the influence of the wind tunnel walls and an excessive blockage of the test section.

Corrections are generally applied if the blockage by the model of the building and its immediate surroundings exceeds about 5% to 10%. Typical geometrical scales used in studies of wind effects on tall structures are about 1:300 to 1:600, while for models of small buildings larger scales in the range of 1:100 may be used. In the current study of a power station chimney a scale of 1:150 was used.

## 3. METHOD

### 3.1. Detail of meshing of the geometry of experimental setup

Fine meshing is used on the inner and outer surface of the chimney and near the bottom area around the chimney. The quality of mesh is above 0.7 in every model. the quality of an element is defined as the determinant of the Jacobian matrix, which is a measure of the element's distortion. The quality of mesh can be checked in ICFM-CFD and if this value is above 0.5 the quality of mesh is referred as good. To get first cell height some calculations are needed as suggested by the CFD package. If Reynolds number is more than  $5 \times 10^5$ , flow over a surface will be turbulent. For most of wind flow problems flow is turbulent.

Now,

$$Re = \frac{\rho v L}{\mu}$$

$$L = 4A/P = (4 \times 1.5 \times 2.65) / 5.65 = 2.81 \text{ m}$$

At Standard Sea Level density,  $\rho = 1.225 \text{ kg/m}^3$

Dynamic viscosity,  $\mu = 1.79 \times 10^{-5} \text{ Pa-s} \approx 1.8 \times 10^{-5} \text{ Pa-s}$

$$Re = \frac{1.225 \times 12 \times 2.81}{1.8 \times 10^{-5}} \\ = 28.68 \times 10^5$$

$Re > 5 \times 10^5$  so flow is turbulent.

Skin friction on a plate,  $C_f = 0.058 \times Re^{-0.2}$

$$= 0.058 \times (28.68 \times 10^5)^{-0.2} \\ = 3.248 \times 10^{-3}$$

$$\tau_w = \frac{1}{2} C_f \rho U^2 = 0.408 \text{ kg/ms}^2$$

U is the free stream velocity (usually taken outside of the boundary layer or at the inlet).

$$U_r = \sqrt{\tau_w / \rho} = 0.557 \text{ m/s}$$

$$y = \frac{y^+ \mu}{U_r \rho} = \frac{150 \times 1.8 \times 10^{-5}}{0.577 \times 1.225}$$

=  $3.8199 \times 10^{-3}$  m. ( $y^+$  is a dimensionless wall unit and it ranges from 30 to 200).

So, take first cell height ( $y$ ) = 4 mm

In Fig 2 and Fig 3, are shown the top view and the side view of isolated chimney model and the chimney model with interference after creating the mesh as per the calculations.

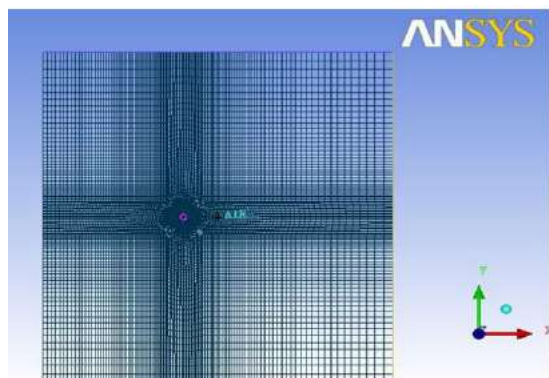


**Figure 2 (a)** Top view of mesh of Isolated chimney model

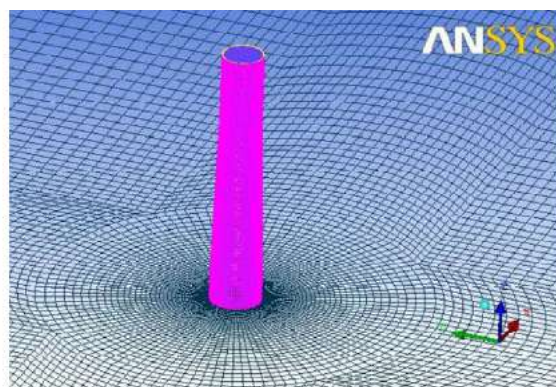


**Figure 2(b)** Side view of mesh of isolated chimney model

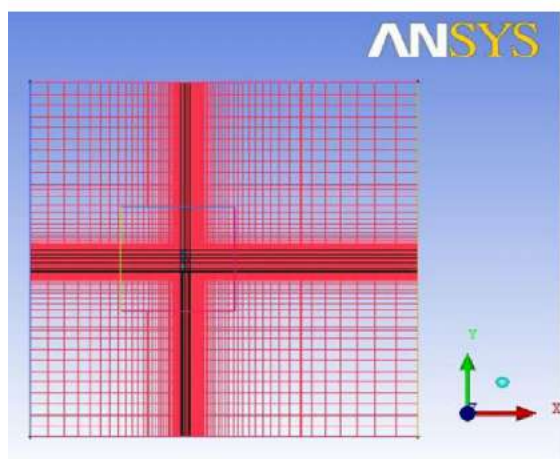


**Figure 3(a)** Top view of mesh of chimney Model with interference

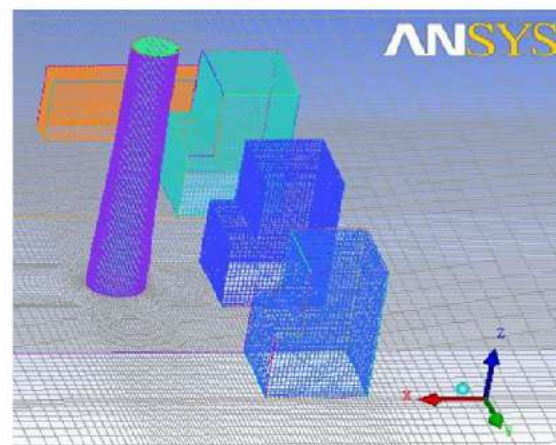


**Figure 3(b)** Top view of mesh of chimney model with interference

## 3.2. Domain Considered for CFD Simulation

### 3.2.1. Isolated Chimney Model

The isolated chimney dimension and dimension for chimney model with interference for CFD simulation are kept the same as the isolated chimney used for the wind tunnel study, i.e., 112mm bottom diameter and 91mm top diameter with a height of 647mm (scaled 1:150).

The wind tunnel cross section (i.e. domain dimensions) taken for the CFD simulation is considered using optimum domain recommendations by Roy A.K

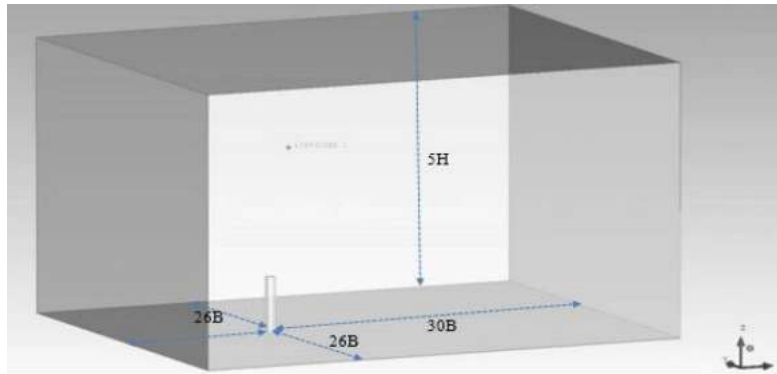


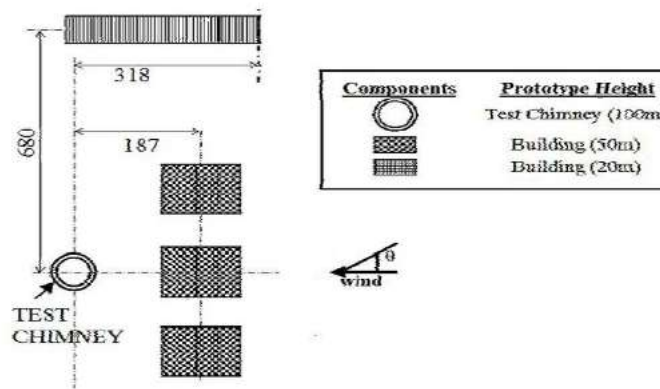
**Figure 4** Computational domain of the isolated chimney model used for CFD simulation

(Roy et al. 2012)

### 3.2.2. Chimney Model with Interference

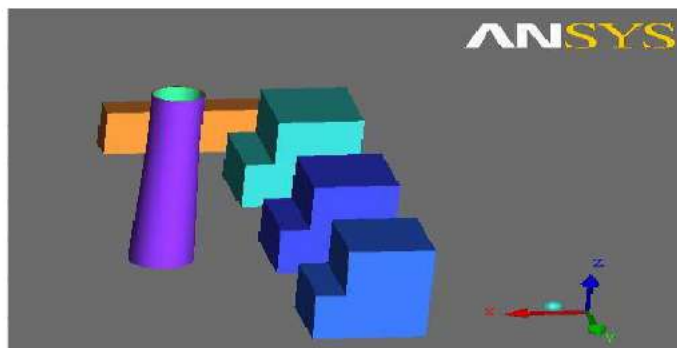
For interference analysis other power station structures are considered near the chimney and the modelling and meshing is then carried out in ICEM-CFD 14.0.

Fig. 5 shows the schematic diagram of the chimney model used along with the other structures



**Figure 5** Schematic diagram of chimney and other structures

The chimney was modelled in ICEM-CFD 14.0 considering the whole chimney as well as the other components as a single block as shown in Fig 4.6 (b) and the domain size as used in an isolated chimney model was altered accordingly.



**Figure 6** Schematic diagram of model used



### 3.3. Turbulence Model

Earlier research workers have already examined different turbulence models for their relative suitability for the atmospheric boundary layer airflow (Blocken, 2007a and 2007b). It has been observed that for this kind of problem the realizable k- $\epsilon$  model (Shih et al., 1995) are most suitable.

The commercial CFD code ANSYS Fluent 14.0.0 (ANSYS Ltd., 2010) is used to solve the 3D Reynolds-averaged Navier–Stokes equations and the continuity equation using the control volume method. Closure is obtained using the realizable k- $\epsilon$  model (Shih, et al. 1995). Pressure–velocity coupling is taken care of by the SIMPLE algorithm. Pressure interpolation is second order. Second-order discretization schemes are used for both the convection terms and the viscous terms of the governing equations.

### 3.4. Boundary Condition

For real physical representation of the fluid flow suitable boundary condition that actually simulate the real flow is required, there is always great difficulty in defining in detail the boundary conditions at the inlet and outlet of the flow domain that is required for accurate solution. At the upwind boundary, a velocity inlet was used with the following expressions for the along-wind component of velocity,  $U$  which is similar to the experimental study. Standard representation of the velocity profile in the ABL is as shown below.

$$U(z) = \frac{u_*}{\kappa} \ln \left( \frac{z + z_0}{z_0} \right) \quad (1)$$

In the present work the values are of the parameters  $z_0 = 0.0002\text{m}$  and  $u_* = 0.11\text{ m/s}$ . The measured longitudinal turbulence intensity ( $I$ ) is converted to turbulent kinetic energy  $k$  as input for the simulations using Eq. (2), assuming that  $\sigma_v \ll \sigma_u$  and  $\sigma_w \ll \sigma_u$ . It is observed that with a higher  $k$ , a small discrepancy in the results in the order of a few percentages (<5%) in the magnitude of amplification factors

$$k(z) = \frac{u_*^2}{\sqrt{C_\mu}} \quad \text{or} \quad k(z) = 0.5(I_U U)^2 \quad (2)$$

The inlet turbulence dissipation rate profile  $\epsilon$  from Richards and Hoxey (1993) is given by

$$\epsilon(z) = \frac{u_*^3}{\kappa(z + z_0)} \quad (3)$$

where,  $z$  is the height co-ordinate,  $\kappa$  the von Karman constant ( $\sim 0.42$ ),  $z_0$  the scaled aerodynamic roughness length corresponding to a power-law exponent of 0.15 (here:  $z_0 = 0.03/150 = 0.0002\text{m}$ ) and  $u_*$  the friction velocity related to a horizontally homogeneous (stable) ABL flow. The sides and the top of the computational domain are modelled as slip walls (zero normal velocity and zero normal gradients of all variables). At the outlet, zero static pressure is specified. The standard coefficients of the realizable k- $\epsilon$  model were used. At the downwind boundary, a pressure outlet was used, with the relative pressure specified at  $0\text{ Pa}$  and backflow conditions for  $k$  and  $\epsilon$  set to those of the inlet. In the domains, however, backflow was not observed because the downwind boundary was sufficiently far from the chimney. On the bottom wall of the domain, a rough wall was specified to model the effect of the ground roughness. The values of  $K_S$  and  $C_S$  are needed as input. According to Blocken et al. (2007a), the roughness constant ( $k_s$ ) in the law of the wall was specified as

$$k_s = \frac{9.793}{C_s} z_0 = 3.98 \times 10^{-3} \quad (4)$$

with  $C_s$  taking its default value of 0.5. The walls of the chimney were specified as smooth. Eqs. (2) to (3) were used to specify the field variables throughout the domain as initial conditions at the start of the steady-state simulation. The standard wall functions modified for roughness are employed. As already specified that for the chosen simulation scale (1/150) the value for  $y_p$  and the reference wind speed  $u_0$  taken from the wind tunnel experiments yields a suitable value of  $y^+$  for the use of wall functions (between 30 and 300).  $K_s$  for the bottom of the computational domain (representing the wind tunnel floor downstream of the roughness elements, including the turntable) is taken  $4 \times 10^{-6}$  m (simulation scale) or 0.0002 m (full scale), which is an estimate of the equivalent sand-grain roughness of the smooth floor. This value is smaller than  $y_p$  (= 0.004 m, simulation scale) as required.

## 4. RESULT AND DISCUSSION

### 4.1. Verification of forces developed on the chimney due to incident wind

#### 4.1.1. IS Code method

The determination of the effective wind pressure is based on the basic wind speed. The basic wind speed ( $V_b$ ) is defined (by the IS:875 (Part3) code) as the mean hourly wind speed at 10m above the ground level in open flat country without having any obstructions. Basic wind speeds generally have been worked out for a return period of 50 yrs.

As per IS:875 (Part-3), the method to calculate the wind forces developed on the structure is defined below:-

#### Basic Design Wind Speed

The design wind speed at the top of the chimney can be obtained from the expression,

$$V_z = k_1 k_2 k_3 V_b$$

Where

$V_z$  = design wind speed at any height  $z$  in m/s

$k_1$  = probability factor (risk coefficient)

$k_2$  = terrain, height and structure size factor

$k_3$  = topography factor

NOTE: Design wind speed up to 10m height from mean ground level shall be considered constant.

#### Design Wind pressure

The design wind pressure at any height above mean ground level shall be obtained by the following relationship between wind pressure and wind velocity:

$$p_z = 0.6 V^2$$

where

$p_z$  = design wind pressure in N/m<sup>2</sup> at height  $z$ , and

$V_z$  = design wind velocity in m/s at height  $z$ .

Note — The coefficient 0.6 (in SI units) in the above formula depends on a number of factors and mainly on the atmospheric pressure and air temperature. The value chosen corresponds to the average appropriate Indian atmospheric conditions.

*Force Resultants*

The pressure values obtained in the earlier case are then converted into the corresponding force values. The chimney is idealized to be a vertical cantilever, fixed to the ground. The load that acts can be taken as continuous load acting on this cantilever. The calculation of the force resultants of shear and moment are trivial. In reality the base of the chimney is broad. Hence the shear resisting capacity of the chimney is high. In fact shear also may manifest itself as moment due to the deep beam effect. Hence the more important resultant to calculate here is the moment as compared to either the shear or the axial force. The force at any point on the cantilever can be calculated by Wind force ;

$$F_z = 0.5 \times C_f \times p_z \times A$$

Where

F = force acting in a direction

$C_f$  = force coefficient for the building

This procedure outlined in the IS:875 specifies the distribution of the value of the drag coefficient around the periphery of the cylindrical shell. This method however does not take into account the effect of the dynamic quality of the incident wind on the chimney.

#### 4.20.1. Calculation of the design wind speed according to IS: 875 Part 3 (1987)

The design wind speed for the chimney is calculated as follows:

Physical Parameters

Height = 97m

Top diameter = 13.60m

Bottom Diameter = 16.80m

Class of structure = C (Structures and/or their components such as cladding, glazing, roofing etc having maximum dimension (greatest horizontal or vertical dimension) greater than 50m.)

Terrain Category = 2 (well scattered obstructions having heights generally between 1.5 to 10 m. It includes the sparsely built up outskirts of towns and suburbs.)

Fig 1 shows the dimensions and the concentrated load profile of the chimney considered for analysis

*Design Wind Speed*

$$V_z = V_b \cdot k_1 \cdot k_2 \cdot k_3$$

Now, For

$z = 97\text{m}$

$V_b = 47\text{m/s}$ ;  $k_1 = 0.9$  ;  $k_2 = 0.79$  ;  $k_3 = 1.0$

$$V_z = V_b \cdot k_1 \cdot k_2 \cdot k_3$$

$= 47 \times 1.07 \times 1.05 \times 1.0 = 33.42 \text{ m/s}$

Now, design wind pressure for  $z = 97\text{m}$

$$p_z = 0.6 V_z^2$$

$$p_z = 0.6 (33.42)^2 = 670.02 \text{ N/m}^2$$

The design pressure values at different elevations are shown below in a tabular form



**Table 1** Design pressure values at different elevations

Elevation (m)	$V_b$ (m/s)	$k_1$	$k_2$	$k_3$	$V_z$ (m/s)	$P_z$ (N/m <sup>2</sup> )
97	47	0.9	0.79	1.0	33.42	670.02
90	47	0.9	0.78	1.0	32.78	644.82
80	47	0.9	0.76	1.0	32.15	620.10
70	47	0.9	0.74	1.0	31.09	579.97
60	47	0.9	0.72	1.0	30.37	553.45
50	47	0.9	0.70	1.0	29.61	526.05
40	47	0.9	0.67	1.0	28.34	481.93
30	47	0.9	0.64	1.0	27.07	439.74
20	47	0.9	0.59	1.0	24.96	373.71
10	47	0.9	0.50	1.0	21.15	268.39

*Force coefficient*

Height/breadth ratio = 97/14.89 (mean average height of the chimney) = 6.51 Considering the surface as rough  $V_d.b \geq 6$  and for this height/breadth ratio the force coefficient (As per Table 23 in IS:875 Part-3)  $C_f$  is 0.8

Wind force calculation

$$F_z = 0.5 \times C_f \times p_z \times A$$

The values of force for different elevations are tabulated below

**Table 2** Values of force for different elevations

z (m)	$C_f$	$P_z$ (N/m <sup>2</sup> )	D (m)	d (m)	A (m <sup>2</sup> )	$F_z$ (N)
97	0.8	670.02	13.6	13	12.5286	3357.753
90	0.8	644.82	13.6	13	12.5286	3231.454
80	0.8	620.10	13.6	13	12.5286	3107.576
70	0.8	579.97	13.6	13	12.5286	2906.492
60	0.8	553.45	14.13	13.53	13.02786	2884.124
50	0.8	526.05	14.65	14.05	13.5177	2844.4012
40	0.8	481.93	15.17	14.57	14.00754	2700.247
30	0.8	439.74	15.7	14.9	19.2168	3380.127
20	0.8	373.71	16.22	15.42	19.86992	2970.244
10	0.8	268.39	16.8	16	20.5984	2211.391

Reaction, shear force and bending moment assuming the chimney as a cantilever beam. The bending moment and shear force are tabulated below for different elevations:

**Table 3** Values of bending moment and shear force at different elevations

Elevation (m)	Bending Moment (N-m)	Shear Force (N)
97	0	3357.753
90	23504.269	6589.206
80	89396.331	9696.782
70	186364.150	12603.274
60	312396.894	15487.398
50	467270.878	18331.800

40	650588.875	21032.046
30	860909.340	24412.173
20	1105031.073	27382.417
10	1378855.245	29593.808

Average value of the shear force acting on the chimney = 30633.938 N

Bending moment about the base = 1674793.324 N-m

Now the bending moment at the base exerted on the structure due to platform weight is tabulated in Table. 4

**Table 4** Bending moment at the base exerted on the structure due to platform weight

z (m)	Platform Weight (kN)	Bending Moment at base due to platforms (N-m)
97	600 kN	$= (600000 \times 97) + (2200000 \times 90) + (300000 \times 70) + (300000 \times 30) + (300000 \times 20)$ $= 292200000$
90	2200 kN	
70	300 kN	
30	300 kN	
20	300 kN	

Total BM at base = (1674793.324 + 292200000) N-m

$$= 293874793 \text{ N-m}$$

$$= 293874 \text{ kN-m} = 2938 \text{ ton-m}$$

Now according to John et al. in Wind induced vibration of scale model of power station chimney - an experimental case study<sup>1</sup>, the bending moment induced at the base of unlined stand-alone chimney calculated by the results from wind tunnel was found out to be 3210 ton-m

#### 4.1.2. Force values from CFD Simulation

The average force acting on the chimney due to wind loads is calculated using the Force function in function calculator available in CFD-Post. This function returns the force exerted by the fluid on the specified 2D locator in the specified direction. The syntax or expression for calculating Force is given below

$$\text{force}[_{\langle \text{Axis} \rangle}[_{\langle \text{Coord Frame} \rangle}] ]()@_{\langle \text{Location} \rangle}$$

where:

<Axis> is x, y, or z

<Coord Frame> is the coordinate frame

<Location> is any 2D region (such as a boundary or interface).

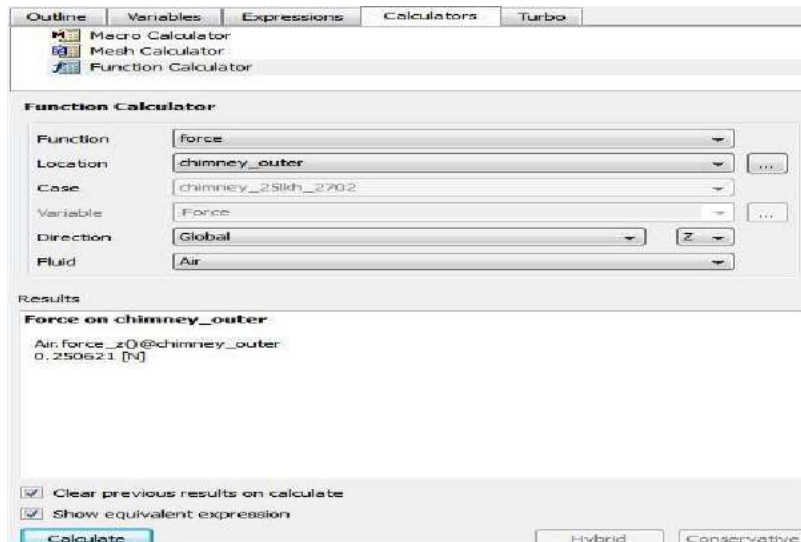
The result as obtained for

#### 4.2. Isolated Chimney

$$\text{Force on chimney\_outer Air.force\_z()}@_{\text{chimney\_outer}}$$

$$0.250621 \text{ [N]}$$

The value obtained is then converted according to the scaling factors used while modelling and simulation stage



Hence,

$$\text{Force} = 0.250621 \times 1000 \times 150 = 37593.15 \text{ N}$$

$$\begin{aligned} \text{Bending moment at base} &= 37593.15 \times \text{average height of building} \\ &= 37593.15 \times 48.5 \\ &= 1823267.775 \text{ N-m} \\ &= 1823 \text{ kN-m} \end{aligned}$$

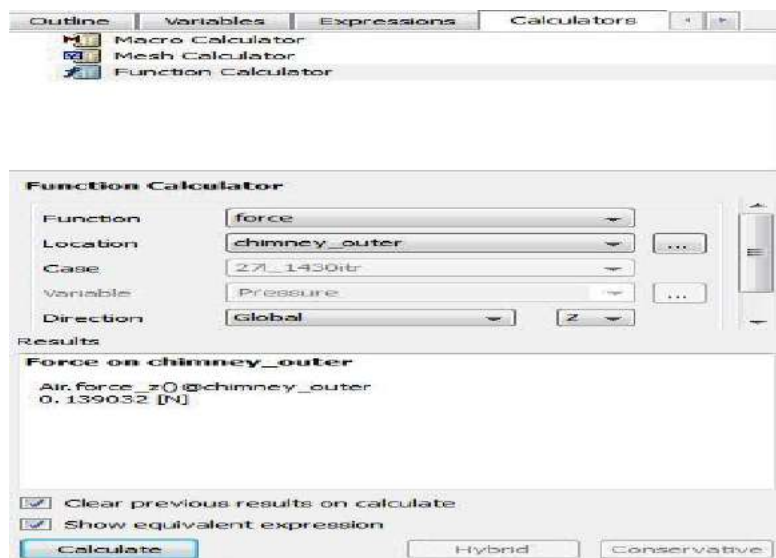
This is comparable to bending moment at base obtained above i.e. 1674793.324 N-m.

$$\begin{aligned} \% \text{ Change in bending moment} &= \frac{1823267.775 - 1674793.324}{1823267.775} \times 100 \\ &= 9\% \end{aligned}$$

Therefore it can be said that the values obtained from IS Code and from CFD-Post are nearly approximate with an error band of 9%.

### 4.3. Chimney Model with Interference

$$\begin{aligned} \text{Force on chimney\_outer Air.force\_z()@chimney\_outer} \\ 0.139032 \text{ [N]} \end{aligned}$$



The value obtained is then converted according to the scaling factors used while modelling and simulation stage.

$$\text{Hence, Force} = 0.139032 \times 1000 \times 150 = 20854.8 \text{ N}$$

$$\begin{aligned} \text{Bending moment at base} &= 20854.8 \times \text{average height of building} \\ &= 20854.8 \times 48.5 \\ &= 1011457.8 \text{ N-m} \end{aligned}$$

Therefore, the bending moment at the base of the chimney in the interference model is 1101457.8 N-m or 1101 kN-m.

$$\begin{aligned} \% \text{ Change in bending moment} &= \frac{1823267.775 - 1101457.8}{1823267.775} \times 100 \\ &= 39.6\% \end{aligned}$$

The bending moment induced at the base of the chimney in case of model with interference is less by 40% than that in the case of isolated chimney model

## 5. REMARK/ CONCLUSION

The use of wind effect on the tall chimney through CFD simulation there are numbers of possibilities of observing the complex wind flow which is the consequence of having a haphazard building orientation around the tall chimney. To find the solution of this complex flow field it is necessary to look into the wind flow pattern around chimney. CFD simulation and the experimental results are very much similar to the experimental study. The accuracy of results depend also on exactly the modelling according to the scale, proper meshing of the model geometry and defining the physical property values exactly as the realistic environment conditions.

## REFERENCES

- [1] Agarwal, S. K., Garg, R. and Lakshmy, P. (1990), "Wind resistant design of structures", *International Journal of Structures*, Vol. 20, No. 1.
- [2] ANSYS Ltd., 2010. Ansys Fluent solver, Release 14.0.0: Theory. Canonsburg.
- [3] Ansys tutorial manuals, Release 14.0.0. Canonsburg.
- [4] Australian standard AS: 1170 Part 2, 1975

- [5] Belver et al. (2012), Lock-in and drag amplification effects in slender line-like structures through CFD.
- [6] Blocken, B. and Carmeliet, J. (2008). Pedestrian wind conditions at outdoor platforms in a high-rise apartment building :generic sub-configuration validation, wind comfort assessment and uncertainty issues. *Wind and Structures*. 11(1) , Pages 51-70.
- [7] Blocken, B., Carmeliet, J., Stathopoulos, T. (2007a), "CFD evaluation of wind speed conditions in passages between parallel buildings – effect of wall-function roughness modifications for the atmospheric boundary layer flow", *Journal of Wind Engineering and Industrial Aerodynamics*, Volume 95, Issues 9–11, Pages 941-962.
- [8] Blocken, B., Stathopoulos, T., Carmeliet, J. (2007b), “CFD simulation of the atmospheric boundary layer: wall function problems”, *Atmospheric Environment*, 41, 238–252.
- [9] Chand I., A low speed wind tunnel for studying the problems on natural ventilation in buildings, *Ind. J. Technology*, 11(1973), 267 - 271.
- [10] Craft. T. J., Trust and quality in CFD. Online teaching material, The university of Manchester. Emil Simiu., Robert H. Scanlan., *Wind effects on structures*.114
- [11] Gartmann et al. (2011), CFD modelling and validation of measured wind field data in a portable wind tunnel. *Aeolian Research* 3 (2011) 315-325.
- [12] IS 875 Part 3 (2007), Code of practice for design loads (other than earthquake) for buildings and structures, *Bureau of Indian Standards*, New Delhi (India).
- [13] IS 4998-1: Criteria for design of reinforced concrete chimneys, Part 1: Assessment of loads (1992), *Bureau of Indian Standards*, New Delhi (India).
- [14] John. A et al. (1992) Wind induced vibration of scale model of power station chimney - *an experimental case study*.
- [15] LeVeque, Randall (2002), Finite Volume Methods for Hyperbolic Problems, *Cambridge University Press*.
- [16] Malay S Patel, Sulochan D Mane and Manikant Raman, Concepts and CFD Analysis of De-Laval Nozzle. *International Journal of Mechanical Engineering and Technology*, 7(5), 2016, pp. 221–240.
- [17] Neil Schlager (1994), When Technology Fails- Significant Technological Disasters, Accidents, and failures of the twentieth century.
- [18] Revuz et al. (2012), On the domain size for the steady-state CFD modelling of a tall building. *Wind and structures*, Vol. 15, No. 4 (2012) 313-329.
- [19] Richards, P.J., Hoxey, R.P., 1993. Appropriate boundary conditions for computational wind engineering models using the k-ε turbulence model. *Journal of Wind Engineering and Industrial Aerodynamics* 46&47, 145-153.
- [20] Sanayei, M., Edgers, L., Alonge, J.L., & Kirshen, P., “Effects of Increased Wind Loads on a Tall Building,” *Civil Engineering Practice*, Vol. 19, No. 1, 2004.
- [21] Ayush Srivastava, Belal Farooqi and Shashi Shekhar Singh, Technique to Determine the Exact Boundary Condition of an Existing RCC Building Slab. *International Journal of Civil Engineering and Technology*, 7(6), 2016, pp.328–334.
- [22] Shenghong huanga,b, q.s. lib, Shengli xua Numerical evaluation of wind effects on a tall steel building by CFD (2007).